Int. J. Solids Structures, 1975, Vol. 11, pp. 575–591. Pergamon Press. Printed in Great Britain

FULLY PLASTIC CRACK PROBLEMS: THE CENTER-CRACKED STRIP UNDER PLANE STRAIN†

N. L. GOLDMAN and J. W. HUTCHINSON
Division of Engineering and Applied Physics, Harvard University, Cambridge, MA 02138, U.S.A.

(*Received* 25 *February* 1974)

Abstract—Crack problems are formulated for solids characterized by a pure power hardening relation between the stresses and the strains. For such problems there are simple functional relationships between the amplitude of the dominant crack-tip singularity, as measured by the path-independent J-integral, and the applied load, the load point displacement, and the crack opening displacement. The solutions are valid for both incremental and deformation theories of plasticity; they also apply to problems involving steady-state creep. Numerical results are presented for the center-cracked strip of finite width under plane strain conditions. A preliminary discussion is given of the applicability of the solutions to large scale yielding fracture mechanics.

INTRODUCTION

The near-tip field at a stationary crack in an elastic-plastic strain hardening material is characterized by a single parameter when the stress field at the crack tip is either symmetric or antisymmetric with respect to the crack and when plane stress or plane strain prevails. Within the context of a small strain deformation theory of plasticity, the amplitude of the dominant singularity governing the stress and strain fields at the crack tip is directly related to Rice's [1] path-independent J-integral, and J can be used as a convenient measure of the strength of the dominant singularity. The potential of this measure in developing a large scale yielding fracture criterion has been demonstrated in a recent series of tests performed by Begley and Landes [2, 3].

For power hardening materials, in which the plastic strain is proportional to the stress raised to a power, the dominant singularity has been studied in some detail [4, 5]. When small scale yielding pertains, J is related to the elastic stress intensity factor by a simple formula. For large scale yielding, J cannot be calculated simply, in general, since it depends in a complicated way on the geometry, load level and nonlinear stress-strain behavior. Notwithstanding, relations between J and such quantities as the crack opening displacement, the load point displacement, and the applied load are required in the implementation of this approach to the fracture analysis of test specimens and cracked bodies in general.

In their pioneering tests, Begley and Landes [2, 3] used an experimental compliance procedure to obtain the relation between J and the load point displacement. More recently, a relatively simple approximate method for estimating the relation between J and the load point displacement has been proposed [6]. This method extrapolates from the small scale yielding range into the fully plastic range using Irwin's plasticity adjustment of the elastic predictions together with results based on a perfect plasticity analysis. Extensive numerical calculations using finite element methods, such as those reported in [7–10], look promising for large scale yielding analysis, but at

†This work was supported in part by the Air Force Office of Scientific Research under Grant AFOSR-73-2476, in part by the Advanced Research Projects Agency under Contract DAHC15-73-G-16, and by the Division of Engineering and Applied Physics, Harvard University.

least one drawback of such calculations is that they must be repeated for essentially every variation in material property or configuration.

Fully plastic crack problems are formulated in this paper for materials whose stress-strain behavior is taken in the form of a pure power hardening relation of the form considered by Ilyushin[11]. For such problems there is an extremely simple functional relationship between J and the applied load or any displacement quantity. The simple form of these solutions suggests that they may prove useful for taking into account strain hardening in extrapolation procedures such as that mentioned above, in addition to providing insight into behavior under fully plastic conditions. Another attractive feature of the fully plastic crack problems is that for applied loads which are monotonically increased the solutions are rigorously valid for both deformation and incremental theories of plasticity. Numerical results are presented for the tensile loading of a center-cracked strip under plane strain conditions.

FORMULATION OF FULLY PLASTIC CRACK PROBLEMS

A small strain formulation of plasticity theory will be used in which the strain-displacement equations and equilibrium equations are the classical linear relations. A pure power hardening relation between stress and strain is assumed so that in simple tension

$$\epsilon/\epsilon_o = \alpha(\sigma/\sigma_o)^n \tag{1}$$

where α is a dimensionless constant, and ϵ_o and σ_o are reference values of the strain and stress. (The connection $\sigma_o = E\epsilon_o$, where E is Young's modulus, can always be made when convenient but need not be introduced here.) With

$$s_{ij} = \sigma_{ij} - \frac{1}{3}\sigma_{pp}\delta_{ij} \text{ and } \sigma_e^2 = \frac{3}{2}s_{ij}s_{ij}$$

the simplest deformation theory (J_2 deformation theory) generalization of (1) is

$$\frac{\epsilon_{ij}}{\epsilon_o} = \frac{3}{2}\alpha\left(\frac{\sigma_e}{\sigma_o}\right)^{n-1}\frac{s_{ij}}{\sigma_o}. \tag{2}$$

Since $\epsilon_{pp} = 0$, the material is inherently incompressible.

If boundary value problems based on (2) are considered where tractions are prescribed on all boundaries, and if the directions of these tractions remain fixed while their magnitudes are everywhere linearly proportional to a single load parameter, then as first shown by Ilyushin[11], the stress at each point in the body also varies linearly with the load parameter. There is no change in the relative proportions of the stress components at each point and therefore the solution is also rigorously correct for the incremental plasticity theory, J_2 flow theory, when the load parameter is monotonically increased. These conditions are clearly satisfied in crack problems where the crack is traction-free and either where tractions on outer boundaries are prescribed proportional to a single parameter or where constant stress condtions are approached at infinity.

In this paper attention is directed to plane strain problems ($\epsilon_{33} = 0$) for Mode I, where the stress field is symmetric with respect to the crack. In this case the stress, strain and displacement fields of the dominant singularity at the crack tip have the form

$$[\sigma_{ij}, \sigma_e] = \sigma_o K_\sigma r^{-[1/(n+1)]} [\tilde{\sigma}_{ij}(\theta), \tilde{\sigma}_e(\theta)]$$
$$\epsilon_{ij} = \alpha \epsilon_o K_\epsilon r^{-[n/(n+1)]} \tilde{\epsilon}_{ij}(\theta) \tag{3}$$
$$u_i = \alpha \epsilon_o K_\epsilon r^{[1/(n+1)]} \tilde{u}_i(\theta)$$

where r is the distance from the crack tip and θ is the angle measured from directly ahead of the crack. The dimensionless functions $\tilde{\sigma}_{ij}(\theta)$, $\tilde{\sigma}_e(\theta)$, $\tilde{u}_i(\theta)$ and $\tilde{\epsilon}_{ij}(\theta)$ depend on the strain hardening exponent n and have been given in [4]. The plastic stress and strain intensity factors, K_σ and K_ϵ, are connected by $K_\epsilon = (K_\sigma)^n$. These amplitudes are given definite meaning by normalizing the maximum value of $\tilde{\sigma}_e(\theta)$ to be unity.

With the strain energy density defined as

$$W = \int_0^{\epsilon_{ij}} \sigma_{kl} \mathrm{d}\epsilon_{kl} = \alpha \sigma_o \epsilon_o \left(\frac{n}{n+1}\right) \left(\frac{\sigma_e}{\sigma_o}\right)^{n+1}$$

the path-independent J-integral for plane problems is given by [1]

$$J = \int_\Gamma (W n_1 - \sigma_{ij} n_j u_{i,1}) \mathrm{d}s \tag{4}$$

where the crack is taken to lie along the x_1 axis and Γ is any contour surrounding the crack tip. The plastic intensity factors are related to J by

$$J = \alpha \sigma_o \epsilon_o K_\sigma K_\epsilon I_n = \alpha \sigma_o \epsilon_o (K_\sigma)^{n+1} I_n = \alpha \sigma_o \epsilon_o (K_\epsilon)^{(n+1)/n} I_n \tag{5}$$

where values of the numerical constant I_n are given for a range of n in [4].†

With a slightly different interpretation the above formulas apply directly to steady, or secondary, creep. For a creep law of the form $\dot{\epsilon}/\epsilon_o = \alpha(\sigma/\sigma_0)^n$ in tension, generalized to multiaxial states by

$$\frac{\dot{\epsilon}_{ij}}{\epsilon_o} = \frac{3}{2} \alpha \left(\frac{\sigma_e}{\sigma_o}\right)^{n-1} \frac{s_{ij}}{\sigma_o},$$

the previous formulas all continue to hold if the strain-like quantities, ϵ_{ij} and K_ϵ, are replaced by their rates, $\dot{\epsilon}_{ij}$ and $\dot{K}_\epsilon$, and u_i is replaced by $\dot{u}_i$. Now W is the strain-rate potential and J continues to play the role of the single parameter characterizing the near-tip stress and strain-rate fields. Thus, from (5), the amplitude of the singularity of the strain-rates at the crack tip is

$$\dot{K}_\epsilon = [J/(\alpha \sigma_o \epsilon_o I_n)]^{n/(n+1)}.$$

The strain-rates are given by (3) and the θ-variations $\tilde{\epsilon}_{ij}(\theta)$ remain unchanged.

The center-cracked strip under plane strain conditions is studied in some detail in this paper. The crack is of length 2a and is centered in a strip of width 2b which is considered to be infinite in extent in the direction normal to the crack (see insert in Fig. 1). For $|x_2| \to \infty$ the in-plane stresses approach $\sigma_{22} = \sigma^\infty$ and $\sigma_{11} = \sigma_{12} = 0$. The edges $x_1 = \pm b$ are taken to be traction-free.

†Since r has length dimensions in (3), $(K_\sigma)^{n+1} = (K_\epsilon)^{(n+1)/n}$ has dimensions of length. If instead, r is taken to be dimensionless, for example the distance from the tip normalized by the half crack length a, then K_σ and K_ϵ are also dimensionless, and in place of (5) one has $J = \alpha \sigma_o \epsilon_o a K_\sigma K_\epsilon I_n$.

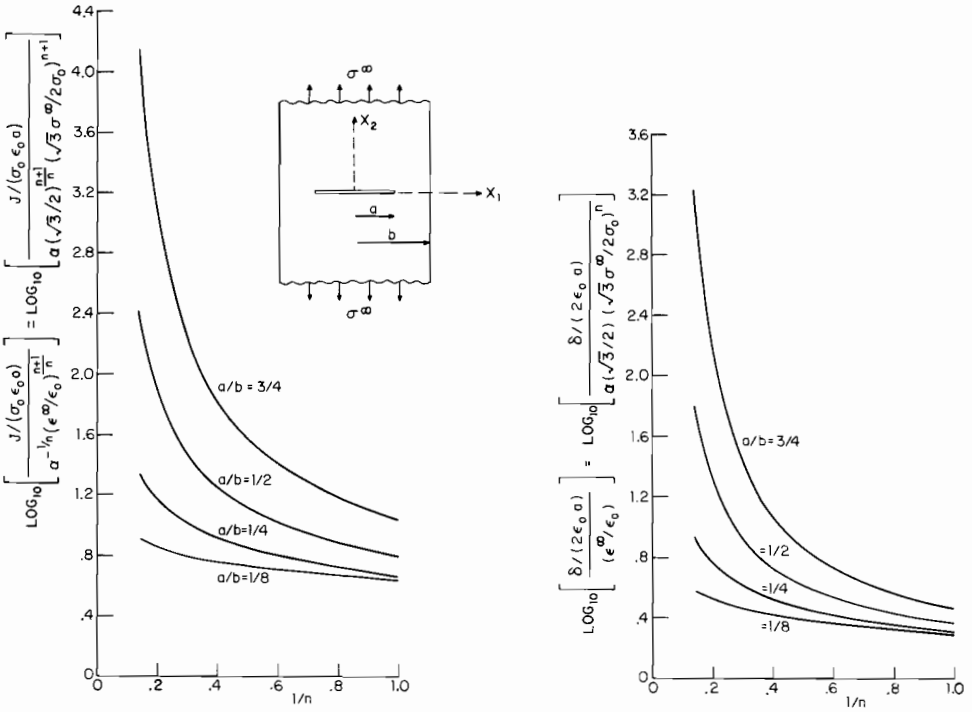

Fig. 1. Curves of J and δ normalized with respect to ϵ^∞ or σ^∞ as a function of $1/n$ for constant values of a/b.

The stresses are linearly related to the applied tractions in a traction boundary value problem in which the material is characterized by (2), as discussed in [11]. The easiest way to see this for a plane problem is to imagine the compatibility equation expressed in terms of a stress function via (2). The resulting equation is homogeneous of degree n in the stress function; and consequently if a given stress field is a solution, then so is any multiple of this same field. It follows then that the functional form of the solution to the fully plastic crack problem is:

$$\begin{aligned} \sigma_{ij}/\sigma_o &= (\sigma^\infty/\sigma_o)\,\hat{\sigma}_{ij}(\mathbf{x}/a, a/b, n) \\ \epsilon_{ij}/\epsilon_o &= \alpha(\sigma^\infty/\sigma_o)^n\,\hat{\epsilon}_{ij}(\mathbf{x}/a, a/b, n) \\ u_i/(\epsilon_o a) &= \alpha(\sigma^\infty/\sigma_o)^n\,\hat{u}_i(\mathbf{x}/a, a/b, n). \end{aligned} \tag{6}$$

In particular,

$$\begin{aligned} J &= \alpha\sigma_o\epsilon_o a(\sigma^\infty/\sigma_o)^{n+1}\,\hat{J}(a/b, n) \\ \delta &= \alpha\epsilon_o a(\sigma^\infty/\sigma_o)^n\,\hat{\delta}(a/b, n) \end{aligned} \tag{7}$$

where $\delta = u_2(x_1 = 0, x_2 = 0^+) - u_2(x_1 = 0, x_2 = 0^-)$ is taken here to be the crack opening displacement at the center of the crack. The dimensionless functions topped by $\hat{}$ are independent of the applied stress σ^∞ and depend only on the parameters a/b and n and, in the case of the field quantities, on the non-dimensional coordinates $\mathbf{x}/a$. It follows from the character of this solution, as expressed by the first equation in (6), that the stress history is proportional at each point so that the solution is valid for J_2 flow theory as well as for J_2 deformation theory.

It is also convenient to introduce the strain approached as $|x_2| \to \infty$. Since plane strain is invoked, for $|x_2| \to \infty$

$$\sigma_{11} \to 0, \sigma_{22} \to \sigma^\infty, \sigma_{33} \to \tfrac{1}{2}\sigma^\infty, \sigma_e \to \tfrac{\sqrt{3}}{2}\sigma^\infty,$$
$$\epsilon_{33} = 0, \epsilon_{22} = -\epsilon_{11} \to \epsilon^\infty \tag{8}$$

and from (2),

$$\frac{\epsilon^\infty}{\epsilon_o} = \alpha \frac{\sqrt{3}}{2}\left(\frac{\sqrt{3}}{2}\frac{\sigma^\infty}{\sigma_o}\right)^n \tag{9}$$

where σ^∞ is considered to be positive.

A finite element method employing a singular crack tip element was used to calculate the quantities $\hat{\sigma}_{ij}$, $\hat{J}$, etc. for a wide range of values of a/b and n. The finite element calculation is complicated by the fact that the material is fully nonlinear and incompressible. The method used is discussed in some detail in the Appendix. We proceed directly to present the results of the calculations in the following section.

NUMERICAL RESULTS FOR THE CENTER-CRACKED STRIP

Normalizations of J and δ which follow from (7) and (9) are

$$\frac{J}{\alpha^{-1/n}\sigma_o\epsilon_o a\left(\frac{\epsilon^\infty}{\epsilon_o}\right)^{(n+1)/n}} = \frac{J}{\alpha\sigma_o\epsilon_o a\left(\frac{\sqrt{3}}{2}\right)^{(n+1)/n}\left(\frac{\sqrt{3}}{2}\frac{\sigma^\infty}{\sigma_0}\right)^{n+1}} = f_1\left(\frac{a}{b}, n\right) \tag{10a}$$

and

$$\frac{\delta}{2\epsilon_o a\left(\frac{\epsilon^\infty}{\epsilon_o}\right)} = \frac{\delta}{2\epsilon_o a\alpha\frac{\sqrt{3}}{2}\left(\frac{\sqrt{3}}{2}\frac{\sigma^\infty}{\sigma_o}\right)^n} = f_2\left(\frac{a}{b}, n\right) \tag{10b}$$

where f_1 and f_2 are non-dimensional functions of a/b and n. Calculated values of f_1 and f_2 are given in Table 1 for combinations of four values of a/b and six values of n ranging from 1 to 7. Over this range of the parameters, values of the non-dimensional combinations in (10) vary by three orders of magnitude as can be seen in the plots of their logarithms as a function of $1/n$ in Fig. 1. Both quantities are unbounded as $a/b \to 1$ for fixed n and are unbounded as $n \to \infty$ for fixed a/b. Cross-plots are shown in Fig. 2.

Before considering normalizations which are more suitable than (10), we will present an appropriate normalization of J in terms of the crack opening displacement at the center of the crack δ. This relation is of some interest, particularly in fracture toughness testing[12]. The relation is known for the limit $n \to \infty$ from the limit analysis of a rigid perfectly plastic center-cracked strip[6]. In this limit,

$$J = (2/\sqrt{3})\sigma_o\delta \tag{11}$$

for all values of a/b. In the limit of linear elasticity, $n = 1$, the normalization

$$\frac{J}{\alpha^{-1}\sigma_o\epsilon_o a\left(\frac{b}{b-a}\right)\left(\frac{\delta}{2\epsilon_o a}\right)^2} \tag{12}$$

Table 1.†

a/b \ n	$n=1$	$n=1{\cdot}5$	$n=2$	$n=3$	$n=5$	$n=7$
$a/b\to 0$	$f_1=4\pi/3$‡ $f_2=2{\cdot}0$‡ $f_3=\pi/3$‡ $f_4=-$ $f_5=4\pi/3$‡ $f_6=2{\cdot}0$‡	$f_3=1{\cdot}25$§	1·37§	1·50§	1·64§	1·76§
$a/b=1/8$	$f_1=4{\cdot}23$ $f_2=1{\cdot}92$ $f_3=1{\cdot}00$ $f_4=0{\cdot}100$ $f_5=3{\cdot}70$ $f_6=1{\cdot}68$	4·97 2·22 1·20 0·129 4·07 1·82	5·46 2·45 1·33 0·154 4·18 1·87	6·02 2·77 1·48 0·211 4·04 1·86	7·08 3·30 1·65 0·314 3·63 1·69	8·15 3·74 1·77 0·408 3·20 1·47
$a/b=1/4$	$f_1=4{\cdot}59$ $f_2=2{\cdot}01$ $f_3=0{\cdot}855$ $f_4=0{\cdot}197$ $f_5=3{\cdot}44$ $f_6=1{\cdot}51$	5·90 2·44 1·10 0·253 3·83 1·58	7·07 2·87 1·26 0·307 3·98 1·61	9·30 3·73 1·46 0·405 3·92 1·57	14·58 5·76 1·69 0·572 3·46 1·37	22·06 8·60 1·81 0·681 2·94 1·15
$a/b=1/2$	$f_1=6{\cdot}24$ $f_2=2{\cdot}31$ $f_3=0{\cdot}586$ $f_4=0{\cdot}396$ $f_5=3{\cdot}12$ $f_6=1{\cdot}15$	9·28 3·11 0·882 0·493 3·28 1·10	13·03 4·12 1·10 0·580 3·26 1·03	24·26 6·97 1·45 0·719 3·03 0·872	80·08 20·41 1·87 0·887 2·50 0·638	264·3 62·80 2·11 0·959 2·06 0·491
$a/b=3/4$	$f_1=10{\cdot}92$ $f_2=2{\cdot}92$ $f_3=0{\cdot}321$ $f_4=0{\cdot}597$ $f_5=2{\cdot}73$ $f_6=0{\cdot}729$	20·73 4·61 0·645 0·726 2·59 0·576	37·28 7·26 0·952 0·821 2·33 0·454	119·2 19·34 1·45 0·932 1·86 0·302	1273·0 170·1 2·03 0·992 1·24 0·116	14040·0 1749·0 2·27 0·999 0·857 0·107

‡Exact value

§Extrapolated value

†Limiting values for $n=1$, $a/b\to 1$ are $f_3=0$ and $f_5=16\pi/[3(\pi^2-4)]$. Limiting values for $n=\infty$ are $f_3=4/\sqrt{3}$ and $f_4=1{\cdot}0$, for all a/b.

leads to a finite limit as $a/b\to 0$ and to a zero limit as $a/b\to 1$. The choice

$$\frac{J}{\alpha^{-(1/n)}\sigma_o\epsilon_o a\left(\dfrac{b}{b-a}\right)^{1/n}\left(\dfrac{\delta}{2\epsilon_o a}\right)^{(n+1)/n}}=f_3\left(\frac{a}{b},n\right) \tag{13}$$

is consistent with (11) and (12) and with the general functional form (7). Calculated values of f_3 are given in Table 1, and are plotted in Fig. 3. Throughout the paper an extrapolated section of a curve in any figure is indicated by a dashed line. In particular, the sections of the curves in Fig. 3a for $n>7$ are extrapolated to the limiting value for $n=\infty$, $f_3=4/\sqrt{3}$, which is known exactly from (11). The curve for $a/b\to 0$ is obtained from extrapolations to this limit shown in Fig. 3b. The temptation to extend the curves in Fig. 3b to $a/b=1$ has been resisted because of uncertainty as to the validity of the geometric singularity $[b/(b-a)]^{1/n}$ introduced in (13).

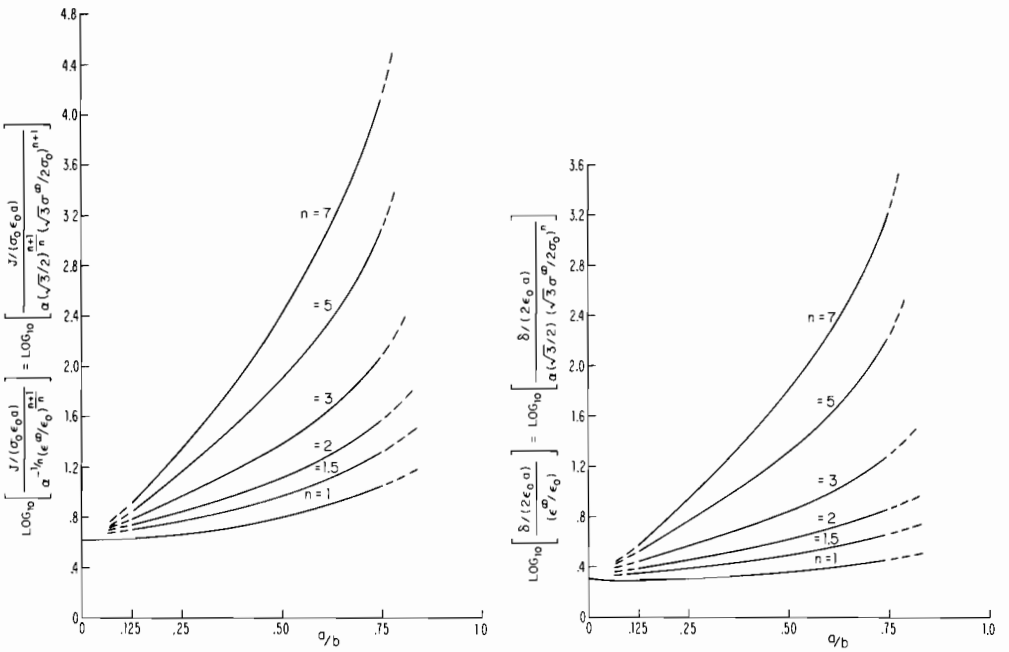

Fig. 2. Curves of J and δ normalized with respect to ϵ^{∞} and σ^{∞} as a function of a/b for constant values of n.

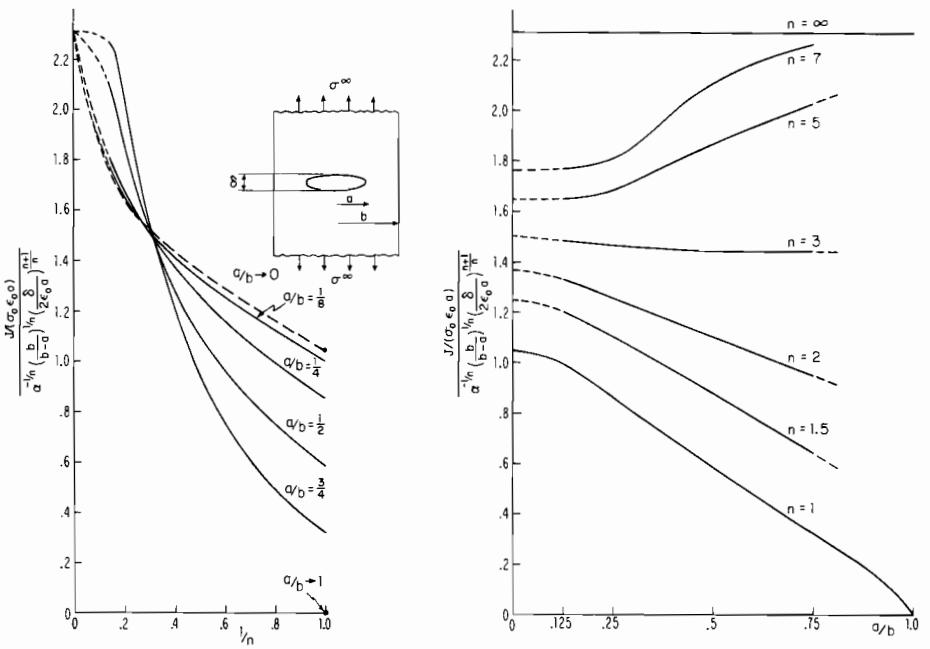

Fig. 3. Curves of J normalized with respect to δ.

Curves showing the displacement normal to the crack normalized by $\delta/2$ are shown in Fig. 4a for $a/b = 1/2$ for several values of n. These curves are independent of σ^∞/σ_o. Under fully plastic conditions for n greater than about 5, the crack opening displacement at the center of the crack is a good approximation to the opening displacement all along the crack, except right at its ends.

Consider a strip of length $2h$ in the x_2 direction, as shown in Fig. 4b, and let $\sigma_{22} = \sigma^\infty$ be applied on $x_2 = \pm h$. Define Δ to be the load point displacement,

$$\Delta = \frac{1}{2b}\int_{-b}^{b} [u_2(x_1, h) - u_2(x_1, -h)]\, dx_1 \tag{14}$$

through which the applied stress does work. In the limit $n \to \infty$, corresponding to rigid perfect plasticity, the deformation is confined to the four 45° shear bands depicted in Fig. 4b, as has been discussed in [13]. In this limit, $\Delta = \delta$, independent of h, as long as h is greater than $b - a$.

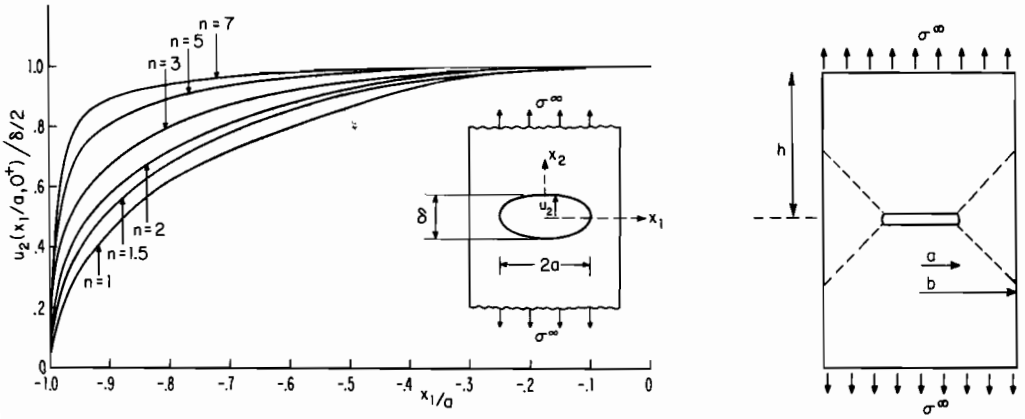

Fig. 4. (a) Crack opening profiles and (b) Geometry for finite length strip showing the slip lines for the rigid perfectly plastic limit.

However, for finite values of the strain hardening exponent, Δ is not independent of the strip length for a given σ^∞, but increases essentially linearly with h once h is sufficiently large compared to a or $b - a$, whichever is relevant. For an uncracked strip of length $2h$ subject to an applied stress σ^∞, the load point displacement is

$$\Delta_{\text{no crack}} = 2h\epsilon^\infty \tag{15}$$

where ϵ^∞ is given by (9). Define a residual load point displacement Δ_R to be

$$\Delta_R = \Delta - \Delta_{\text{no crack}}. \tag{16}$$

For sufficiently large h, Δ_R is essentially independent of h; for $n \to \infty$, $\Delta_R = \Delta = \delta$. For a finite value of n and a given applied stress σ^∞, Δ can be obtained from (16) if Δ_R is known.

The relationship between Δ_R and δ is shown in Fig. 5. As discussed in the Appendix, the values of h/b chosen in carrying out the calculations were sufficiently large to ensure that the values of Δ_R presented are the limit values for $h \to \infty$, within the accuracy of the numerical

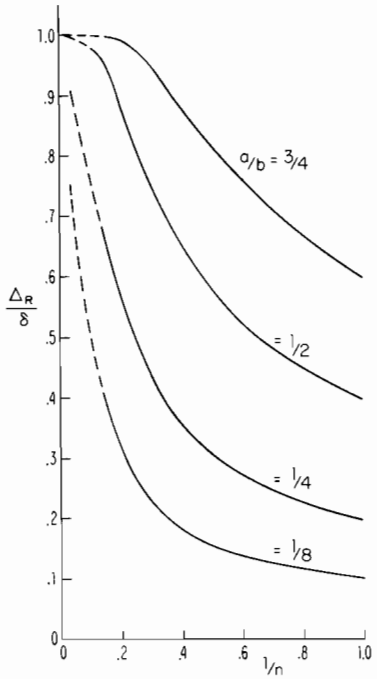

Fig. 5. Ratio of residual load point displacement to crack opening displacement at center of crack.

method. Values of the function f_4, where

$$\frac{\Delta_R}{\delta} = f_4(a/b, n) \tag{17}$$

are given in Table 1. While $\Delta_R = \delta$ in the limit of perfect plasticity ($n = \infty$), a very small amount of strain hardening significantly alters this relation when a/b is less than about 1/2. An expression for J in terms of Δ_R can be obtained simply by using (17) to eliminate δ in (13).

It is a more delicate matter to choose a suitable normalization of J with respect to ϵ^∞ or σ^∞. The normalizations (10) used in Figs. 1 and 2 do not incorporate any a/b dependence and this leads to a very strong dependence of f_1 and f_2 on a/b. For linear elasticity ($n = 1$) a normalization of the form

$$\frac{J}{\alpha\sigma_o\epsilon_o a[b/(b-a)](\sigma^\infty/\sigma_o)^2} \tag{18}$$

has finite limits for $a/b \to 0$ and for $a/b \to 1$ which are known exactly[14].

The net section stress acting across the ligament on either side of the crack is $\sigma_{net} = \sigma^\infty b/(b-a)$. The following limits are approached as $n \to \infty$ in the ligament regions on either side of the crack:

$$\sigma_e \to \sigma_o \text{ and } \sigma_3 \to \sqrt{(3)}\,\sigma_{net}/2 \Rightarrow \sigma_{net} \to 2\sigma_o/\sqrt{3}.$$

From (7), J is proportional to stress raised to the $(n+1)^{th}$ power. Tentatively consider a normalization based on the net ligament stress, i.e.

$$\frac{J}{\alpha\sigma_o\epsilon_o a\left(\frac{\sqrt{3}}{2}\frac{\sigma_{net}}{\sigma_o}\right)^{n+1}} = \frac{J}{\alpha\sigma_o\epsilon_o\left(\frac{b}{b-a}\right)^{n+1}\left(\frac{\sqrt{3}}{2}\frac{\sigma^\infty}{\sigma_o}\right)^{n+1}} \tag{19}$$

which clearly is consistent with the general functional form of the solution (7). To bring (19) in line with (18) for $n = 1$, multiply it by $b/(b-a)$. Also divide (19) by $(\sqrt{3}/2)^{(n+1)/n}$ to arrive at the final form of the normalization to be used in this paper

$$\frac{J}{\alpha\sigma_o\epsilon_o a\left(\frac{b}{b-a}\right)^n\left(\frac{\sqrt{3}}{2}\right)^{(n+1)/n}\left(\frac{\sqrt{3}}{2}\frac{\sigma^\infty}{\sigma_o}\right)^{n+1}} = \frac{J}{\alpha^{-1/n}\sigma_o\epsilon_o a\left(\frac{b}{b-a}\right)^n\left(\frac{\epsilon^\infty}{\epsilon_o}\right)^{(n+1)/n}} = f_5(a/b, n). \tag{20}$$

The normalization for the crack opening displacement is taken to be

$$\frac{\delta/(2\epsilon_o a)}{\alpha\left(\frac{b}{b-a}\right)^n\frac{\sqrt{3}}{2}\left(\frac{\sqrt{3}}{2}\frac{\sigma^\infty}{\sigma_o}\right)^n} = \frac{\delta/(2\epsilon_o a)}{\left(\frac{b}{b-a}\right)^n\left(\frac{\epsilon^\infty}{\epsilon_o}\right)} = f_6(a/b, n). \tag{21}$$

Numerical values for f_5 and f_6 are included in Table 1 and are plotted as solid lines in Fig. 6.

These normalizations are clearly successful in scaling the curves. They emphasize the extremely strong influence of geometry on the relation between J and the stress or strain at infinity when n is large. However, they do not permit an extrapolation to values of n greater than about 10, corresponding to low strain hardening. Neither do they permit an accurate extrapolation to $a/b = 0$, the limit of a finite crack in an infinite body.

Some closely related results for the fully plastic problem in anti-plane shear (Mode III) are available. Amazigo[15] considered a finite crack of half-length a in an infinite body. A pure power hardening law analogous to (1) was assumed, i.e.

$$\gamma/\gamma_o = \alpha(\tau/\tau_o)^n,$$

and was generalized using the analog of (2). The results of Amazigo's exact solution to this problem are displayed in Fig. 7. The functional form of the solution is the same as in (7) with $a/b = 0$. For large n Amazigo found

$$\frac{J}{\alpha^{-1/n}\tau_o\gamma_o a(\gamma^\infty/\gamma_o)^{(n+1)/n}} \cong \frac{\delta}{a\gamma^\infty} \cong 0(\sqrt{n}) \tag{22}$$

where here the crack opening displacement δ is taken as the relative displacement of the two faces of the crack at its center. The relation of J to δ approaches the perfect plasticity result $J = \tau_o\delta$ as $n \to \infty$, as can be seen in Fig. 7b. This curve is very similar to the corresponding curve (a/b$\to$0) in Fig. 3a for the plane strain problem.

The curves of Fig. 1 indicate unbounded behavior. On the other hand, the normalizations (10) and (21) plotted in Fig. 6 appear to be heading to zero as $n \to \infty$ for each fixed, non-zero value of a/b. This is due to the geometric factor $[b/(b-a)]^n$ used in (20) and (21) which, for any non-zero

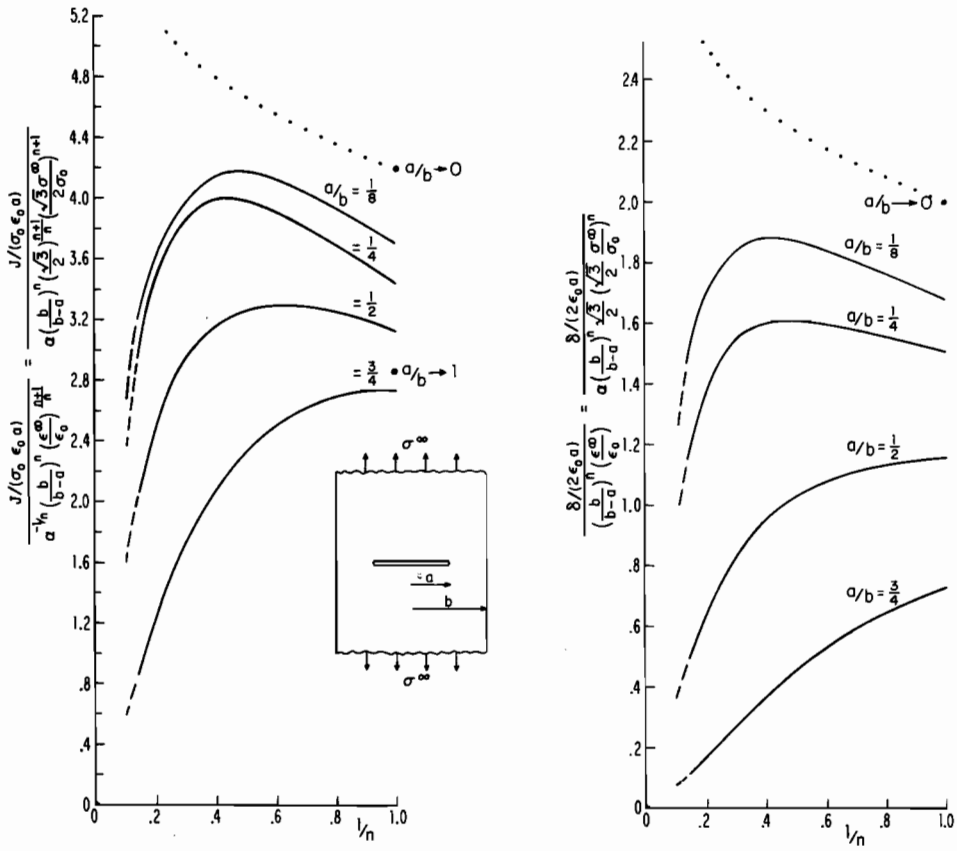

Fig. 6. Curves of J and δ normalized with respect to ϵ^∞ or σ^∞ which incorporate dependence on the geometric parameter a/b. Dotted line curves for $a/b \to 0$ indicate expected qualitative behavior.

value of a/b, appears to dominate the normalizations for large n. Guided by the anti-plane shear results and the above observations, we speculate that the dotted curves in Fig. 6 represent the *qualitative* behavior for the limiting case $a/b \to 0$. Additional attempts to extrapolate the numerical results using normalizations which incorporated large n behavior, such as in (22), did not meet with success. The fact that it did not prove possible to extrapolate the results much beyond the range in which numerical calculations were made is not entirely surprising. Even in a much simpler problem of this type—the axisymmetric deformation around a hole in a sheet subject to biaxial tension—where an exact solution has been found[16], the functional dependence on n alone is quite complicated.

In summary, we feel confident that the curves relating J to δ of Fig. 3, including the extrapolations, are accurate to within a few per cent. In contrast, we were not able to extend the relation of J to ϵ^∞ (or δ to ϵ^∞) to values of n much greater than the largest computed value, $n = 7$; nor could this relation be extended to the limit $a/b = 0$ with acceptable accuracy.

IMPLICATIONS FOR FRACTURE ANALYSIS

In testing for the critical value of J under plane strain conditions, J_{Ic}, the methods used to date involve the experimental determination of the value of some displacement quantity associated

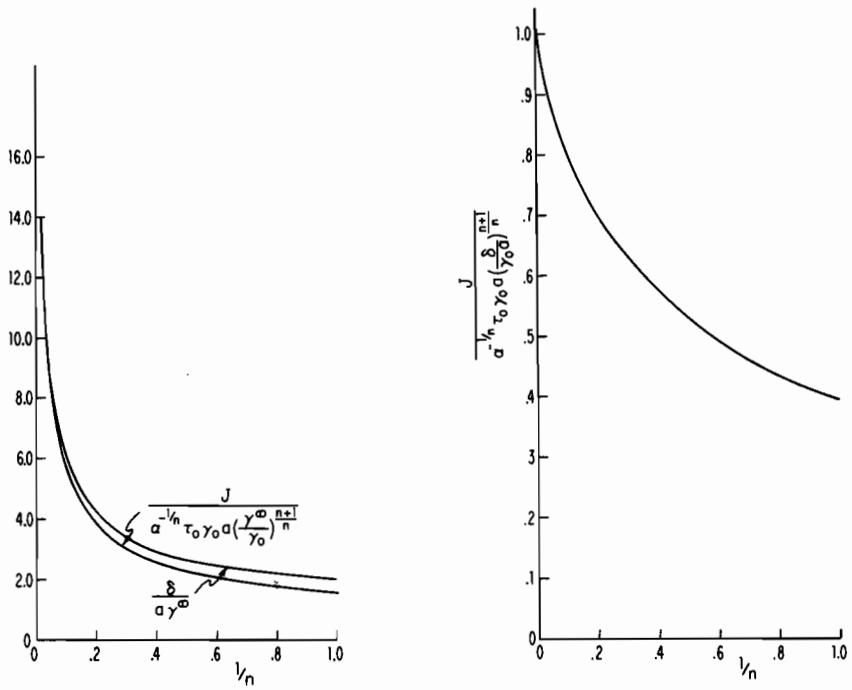

Fig. 7. Results for the finite crack in an infinite body under anti-plane shear (Amazigo[15]).

with the onset of plane strain fracture. Assuming the dependence of J on this displacement quantity is known, J_{Ic} can then be obtained. The load point displacement has been used for this purpose. Various crack opening choices have also been used. As mentioned in the Introduction, an attractive, relatively simple procedure has been proposed [6], which makes use of rigid perfectly plastic results for cracked bodies, to extrapolate predictions from the small scale yielding range into the large scale yielding range. Fully plastic solutions, such as those discussed here, can be employed in carrying out this extrapolation when strain hardening is significant.

To illustrate the extent to which strain hardening can be expected to influence the relation between J and δ in the fully plastic range, consider a finite crack of half-length a in an infinite body. Take δ to be the crack opening displacement as defined in this paper. According to the fully plastic solution (13)

$$\frac{J}{\sigma_o \epsilon_o a} = f_3(0, n)\alpha^{-1/n}\left(\frac{\delta}{2\epsilon_o a}\right)^{(n+1)/n} \tag{23}$$

where $f_3(0, n)$ is the ordinate of Fig. 3a for the curve $a/b = 0$. For $n \to \infty$, (23) reduces to the perfect plasticity result $J = 2\sigma_o\delta/\sqrt{3}$. Curves of $J/(\sigma_o\epsilon_o a)$ as a function of $\delta/(2\epsilon_o a)$ calculated from (23) with $\alpha = 1$ for $n = 3$, 10 and ∞ are shown in Fig. 8a. The extrapolation method of [6] makes use of the slope of the $J - \delta$ relation, $dJ/d\delta$, rather than the relation itself, and Fig. 8b shows the extent to which this slope depends on n. Using (23),

$$\frac{dJ/d\delta}{2\sigma_o/\sqrt{3}} = \alpha^{-1/n}\frac{\sqrt{3}}{4}\left(\frac{n+1}{n}\right) f_3(0, n)\left(\frac{\delta}{2\epsilon_o a}\right)^{1/n}. \tag{24}$$

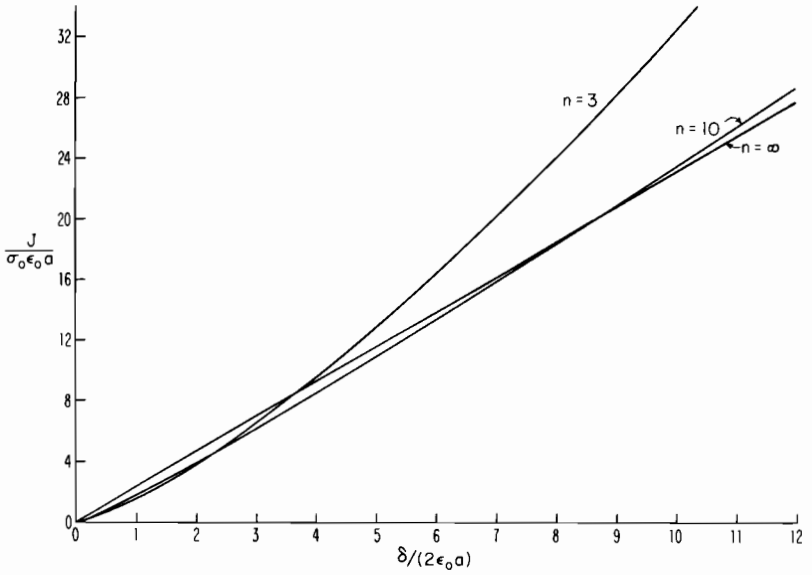

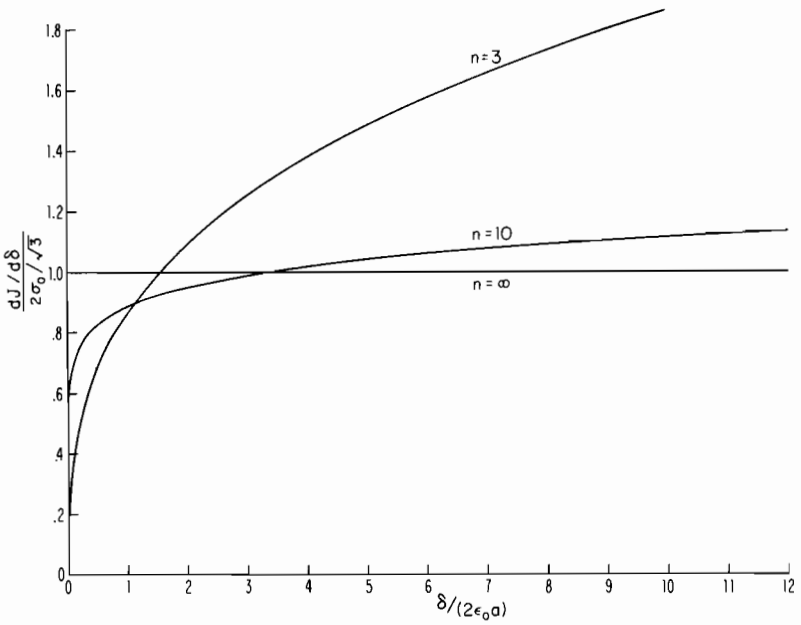

Fig. 8. Curves of J and $dJ/d\delta$ as a function of the crack opening displacement, as predicted by the fully plastic solution for a finite crack in an infinite body with $\alpha = 1$.

For $a/b = 0$ and $\alpha = 1$, the effective stress at infinity reaches σ_o, corresponding to complete yielding in an actual situation, when, from (9), $\epsilon^\infty = \sqrt{(3)}\,\epsilon_o/2$. Thus from Fig. 6b, the corresponding value of $\delta/(2\epsilon_o a)$ will be greater than approx. 2. One can conclude from the curve for $n = 10$ in Fig. 8a that, as long as $n \geq 10$, the $J - \delta$ relation is closely approximated by the perfect plasticity prediction in the range $2 < \delta/(2\epsilon_o a) < 10$. The perfect plasticity prediction for $dJ/d\delta$ differs from the $n = 10$ results by no more than 10 per cent in this same range. For a high strain hardening material as typified by $n = 3$, the discrepancy is considerable.

Under conditions of constrained plastic deformation the overall strain at fracture may be of primary interest. For example, suppose a crack is sufficiently small such that fracture initiation does not occur before the region surrounding the crack becomes fully plastic. Then it may be of interest to ask how large must the "applied" or overall strain be for J to reach J_{Ic}. For a crack of length 2a in an infinite body under fully plastic plane strain conditions, (20) gives

$$\frac{J}{\sigma_o \epsilon_o a} = \alpha^{-1/n} f_5(0, n) \left(\frac{\epsilon^\infty}{\epsilon_o}\right)^{(n+1)/n} \tag{25}$$

where $f_5(0, n)$ is the ordinate of Fig. 6a for the curve $a/b = 0$. (As $n \to \infty$, $f_5(0, n) \to \infty$; even in the range $3 < n < 7$ no claim is made for the accuracy of this curve, as previously discussed.) Solving (25) for the critical applied strain ϵ_c^∞ in terms of J_{Ic} gives

$$\frac{\epsilon_c^\infty}{\epsilon_o} = \left[\frac{\alpha^{1/n} J_{Ic}}{f_5(0, n)\sigma_o \epsilon_o a}\right]^{n/(n+1)}. \tag{26}$$

For all but extremely high strain hardening, the exponent $n/(n+1)$ is almost unity, so the critical strain varies essentially as the inverse of the crack length in the fully plastic range.

To continue the illustration, consider the pressure vessel steel, A553B, used in the Begley-Landes tests [2] for which a J_{Ic} of approximately 1000 in-lbs/in^2 was found. Identify σ_o with the 0·2 per cent offset yield stress, 70 ksi, ϵ_o with the associated yield strain $2{\cdot}3 \times 10^{-3}$, and take $n = 14$, corresponding to the strain hardening exponent of the metal. As a rough estimate for a finite crack in an "infinite" body ($a/b = 0$) use the value $f_5(0, 14) \cong 6$. With $\alpha^{1/n} \cong 1$, (26) predicts that the applied strain at fracture initiation ϵ_c^∞ will exceed the yield strain ϵ_o for all cracks which have a half crack length of approximately one inch or less.

CONCLUDING REMARKS

The fully plastic solutions for the pure power hardening material have the property that the stress history at each point is proportional and, as previously emphasized, represent exact solutions to J_2 flow theory and J_2 deformation theory. In general this will not be true, for example, for a solid characterized by a piecewise power hardening tensile stress-strain curve, made up of linear and nonlinear portions.

There are several possible ways to use the fully plastic strain hardening solutions to extrapolate behavior for small scale yielding to large scale yielding, based on realistic tensile stress-strain curves involving both elastic and plastic strains. The method proposed by Bucci *et al.* [6] for elastic perfectly plastic solids is one of them. A discussion of this subject will be taken up in a subsequent paper.

For the center-cracked strip, the relation between the amplitude of the dominant singularity J and the applied stress σ^∞ or the applied strain ϵ^∞ is highly sensitive to the hardening exponent n and to the geometric parameter a/b. As has been discussed earlier, there are important gaps in the

relationship which remain to be computed accurately, particularly in the range of low strain hardening. It should be noted, however, that for steady-state creep applications the range of n of interest has been covered.

REFERENCES

1. J. R. Rice, Mathematical analysis in the mechanics of fracture, in *Fracture*. pp. 191–311. (Edited by H. Liebowitz), Vol. II, Academic Press, New York (1968).
2. J. A. Begley and J. D. Landes, The J integral as a fracture criterion, in *Fracture Toughness*, pp. 1–20. ASTM STP 514, American Society for Testing and Materials, Philadelphia (1972).
3. J. D. Landes and J. A. Begley, The effect of specimen geometry on J_{Ic}, in *Fracture Toughness*, pp. 24–39. ASTM STP 514, American Society for Testing and Materials, Philadelphia (1972).
4. J. W. Hutchinson, Singular behavior at the end of a tensile crack in a hardening material, and Plastic stress and strain fields at a crack tip, *J. Mech. Phy. Solids* **16**, 13, 337 (1968).
5. J. R. Rice and G. F. Rosengren, Plane strain deformation near a crack tip in a power-law hardening material, *J. Mech. Phy. Solids* **16**, 1 (1968).
6. R. J. Bucci, P. C. Paris, J. D. Landes and J. R. Rice, J integral estimation procedures, in *Fracture Toughness*, pp. 40–69. ASTM STP 514, American Society for Testing and Materials, Philadelphia (1972).
7. P. D. Hilton and J. W. Hutchinson, Plastic intensity factors for cracked plates, *Eng. Frac. Mech.* **3**, 435 (1971).
8. J. R. Rice and D. M. Tracey, Computational fracture mechanics, in *Numerical and Computer Methods in Structural Mechanics* (Edited by S. J. Fenves *et al.*). Academic Press, New York (1973).
9. H. Andersson, Finite-element analysis of a fracture toughness test specimen in the non-linear range, *J. Mech. Phys. Solids* **20**, 33 (1972).
10. D. J. Hayes and C. E. Turner, An application of finite element techniques to post-yield analysis of a practical fracture test specimen, *Int. J. Frac.* to be published.
11. A. A. Ilyushin, The theory of small elastic-plastic deformations, *Prikadnaia Matematika i Mekhanika, P.M.M.* **10**, 347 (1946).
12. A. A. Wells, Crack opening displacements from elastic-plastic analyses of externally notched tension bars, *Engng Frac. Mech.* **1**, 399 (1969).
13. F. A. McClintock, Plasticity aspects of fracture, in *Fracture* (Edited by H. Liebowitz), Vol. III, pp. 47–225. Academic Press, New York, (1971).
14. J. P. Benthem and W. T. Koiter, Asymptotic approximations to crack problems, in *Mechanics of Fracture I* (Edited by G. C. Sih). Noordhoff Leyden (1973).
15. J. C. Amazigo, *Fully plastic crack in an infinite body under anti-plane shear. Int. J. Solids Struc.* **10**, 1003 (1974).
16. B. Budiansky, An exact solution to an elastic-plastic stress-concentration problem, *P.M.M.*, **35**, 1 (1971).
17. N. L. Goldman, *Fully Plastic Crack Problems*, Ph.D. Thesis, Harvard University (Dec. 1973).

APPENDIX

In this Appendix, some of the features of the numerical method will be discussed. Further details are presented[17].

The incompressibility of the material leads to a simplified analytical formulation but complicates the numerical procedure. After careful consideration of several possible ways to treat the incompressible plane strain problem, including the use of Lagrangian multipliers and the use of a displacement potential, an extrapolation technique was chosen because it appeared, at least at the outset of the investigation, to be the most economical approach. In this method, compressibility was introduced in a nonlinear manner in order to preserve the pure power hardening nature of the constitutive relation. The generalized stress-strain relation (2) was modified as

$$\frac{\epsilon_{ij}}{\epsilon_o} = \frac{3}{2}\alpha\left(\frac{\sigma_e}{\sigma_o}\right)^{n-1}\frac{s_{ij}}{\sigma_0} + \frac{1}{3}\beta\left(\frac{\sigma_h}{\sigma_o}\right)^{n-1}\frac{\sigma_{kk}}{\sigma_o}\delta_{ij} \tag{A1}$$

where $\sigma_h \equiv \sqrt{(\sigma_{kk}^2)} = |\sigma_{kk}|$, and β is a positive parameter used to adjust the level of compressibility. In simple tension (A1) reduces to $\epsilon/\epsilon_o = (\sigma/\sigma_o)^n(\alpha + 1/3\,\beta)$. The incompressible limit will be attained by extrapolion to $\beta = 0$.

The nonlinear stress boundary value problem was formulated in terms of the variational principle of minimum potential energy, and solved numerically by a finite element method which makes use of a singular crack tip element. This procedure, similar to the one developed in [7], involves embedding the dominant singularity solution (3) into a finite element grid using a singular tip element centered at the crack tip. The singular element or core region, of radius r_1 with boundary Γ_1, must be sufficiently small for the asymptotically correct dominant singularity solution to accurately represent the near-tip behavior. The displacements at the nodes on Γ_1, from (3), are

$$u_i = \alpha\epsilon_o K_\epsilon r_1^{1/(n+1)}\tilde{u}_i(\theta) + u_o\delta_{i1} \tag{A2}$$

where a rigid-body translation parameter u_o must be included to allow for horizontal displacement of the crack tip and core region. The finite element method was used to describe the solution outside the core region and conventional constant strain triangular elements were employed.

The two-dimensional potential energy functional is defined by

$$\Omega = \int_A W\mathrm{d}A - \int_{S_T} \bar{T}_i u_i \mathrm{d}s \tag{A3}$$

where W is the strain energy density, and S_T is the portion of the boundary on which the tractions $\bar{T}_i$ are prescribed.

Symmetry conditions permit consideration of the first quadrant of the body and the potential energy per unit thickness of this region can be constructed as

$$\Omega = U_c + \sum_{k=1}^{M} U^{(k)} - \sigma^\infty \int_0^b u_2(x_1, h)\mathrm{d}x_1 \tag{A4}$$

where U_c and $U^{(k)}$ represent the strain energies per unit thickness of the core region and of element (k), respectively, and M is the total number of elements in the grid pattern.

From the dominant singularity solution, U_c can be calculated as

$$U_c = \alpha\sigma_o\epsilon_o \frac{n}{n+1} K_\epsilon^{(n+1)/n} r_1 \int_0^\pi [\tilde{\sigma}_e(\theta)]^{n+1}\,\mathrm{d}\theta \tag{A5}$$

The strain energy in the k^{th} element $U^{(k)}$, calculated from (A1) is

$$U^{(k)} = \sigma_o\epsilon_o \frac{n}{n+1}\left[\alpha^{-1/n}\left(\frac{e_\varepsilon}{\epsilon_o}\right)^{(n+1)/n} + \frac{1}{3}\beta^{-1/n}\left(\frac{e_h}{\epsilon_o}\right)^{(n+1)/n}\right]A_k \tag{A6}$$

where

$$e_{ij} = \epsilon_{ij} - \frac{1}{3}\epsilon_{kk}\delta_{ij}$$

$$e_e = \sqrt{\left(\frac{2}{3}e_{ij}e_{ij}\right)} = \alpha\sigma_e^n$$

$$e_h = \sqrt{\epsilon_{kk}^2} = \beta\sigma_h^n$$

and A_k is the area of the element. The energy in the core was calculated using the singularity fields for the incompressible material rather than (A1). Numerical experimentation for the linear

elastic case ($n = 1$), using an incompressible core element in one case and a proper compressible core element consistent with (A1) in another, indicated that the extrapolated results for the $\beta = 0$ limit were essentially the same. The differences were considerably smaller than errors inherent to the grid of the finite element method. The procedures for treating the boundary traction integral in (A4) and the zero displacement boundary conditions, were straightforward and will not be commented upon.

The undetermined parameters of this formulation are K_ϵ and u_o, associated with the singular tip element, and the displacements $\hat{u}_m$ ($m = 1$–$2N$) of the N nodal points which do not lie on Γ_1. Minimizing the potential energy functional with respect to these parameters yields the following governing system of nonlinear equations:

$$\frac{\partial \Omega}{\partial K_\epsilon} = 0, \frac{\partial \Omega}{\partial u_o} = 0, \frac{\partial \Omega}{\partial \hat{u}_m} = 0. \tag{A7}$$

This nonlinear system was solved iteratively by Newton's method. The symmetric, banded, linear system of equations for the corrections δK_ϵ, δu_o and $\delta \hat{u}_m$, was solved by a Gaussian elimination scheme employing triangular decomposition. Because of the highly nonlinear nature of the problem, convergent solutions for $n \geq 2$ were best obtained by adding only a fraction of the calculated Newton increment to the previous guess solution at each stage of the iterative process. The initial displacement solution used in the Newton process was taken to be the linear elastic solution corresponding to $n = 1$. It was convenient to obtain solutions for successive increasing values of n by using the preceding solution as the starting point. Similarly, for constant n, solutions were obtained for decreasing values of β. Calculations using hardening exponents above seven required progressively more iterations to obtain convergence, and, in addition, there was evidence that the accuracy of the method was deteriorating.

Numerical experimentation based on the linear elastic problem was used to check the accuracy of the overall method, to experiment with various grid networks, and to make appropriate choices of grid parameters such as the core radius and the strip length. There was no difficulty in obtaining the strain intensity factors for the incompressible problem by linearly extrapolating to $\beta = 0$. Since the stiffness matrix with $\beta = 0$ is singular, the calculation procedure broke down due to round-off error as β approached this limit, but this problem was bypassed by the extrapolation. The solutions for K_ϵ extrapolated to the incompressible limit agree to within four per cent with the values given in [14], which are claimed to be accurate to one per cent.

Solutions were obtained for combinations of four crack length to specimen width ratios, $a/b = 1/8$, $1/4$, $1/2$ and $3/4$, and six values of n ranging from 1–7. Computations were performed with a grid pattern consisting of 736 elements, 400 nodal points, 13 nodes on Γ_1, and a value of r_1 typically equal to 2·5 per cent of the half crack length. The strain intensity factor was found to be relatively insensitive to the vertical dimension for $h/a \geqq 5$, and this value is consistent with values reported in the literature.

The same grid was used in the nonlinear cases. For each a/b ratio considered, $h/b \geq 1 - a/b$, which ensured that results were independent of h in the limit $n = \infty$. It became progressively more difficult to carry out extrapolations to $\beta = 0$ as n increased, and it is felt that in general, the accuracy achieved for large n is not quite as good as in the linear elastic cases.

The most unsatisfactory aspect of the numerical procedure, in retrospect, was the difficulty involved in extrapolating to the incompressible limit. It may well be that other methods, such as those mentioned earlier, would prove to be better suited to the numerical analysis of this class of problems, and these should be explored.